

INVESTIGATION OF HIGH-SPEED AIR JETS OF AN
EXPLOSIVE PLASMA GENERATOR

Yu. N. Kiselev, V. B. Rozhdestvenskii,
G. S. Romanov, K. L. Samonin, and V. V. Urban

UDC 533.6.09+535.231.6

Of the various facilities that transform energy of an explosion into energy of a dense plasma jet, the explosive plasma generator (EPG) [1] has definite advantages. With the aid of the high energy jets of this facility sources of high-power continuum radiation have been created [2-4], strong shock waves in gases have been investigated [5], and heat treatment of metal surfaces has been carried out [6]. The complexity of the physical processes occurring in the operation of the EPG require study by theoretical and experimental methods. The present paper gives results of experimental and theoretical investigations of the EPG with a compression chamber in the form of a spherical segment of radius 5 cm and base diameter 9.6 cm, filled with 0.2 g of air at 0.1 MN/m^2 . A shock projectile in the form of a flat plate of aluminum of thickness 2 mm was accelerated by an explosive charge of density 1.71 g/cm^3 and energy 3.34 MJ.

The arrangement of the experiment is analogous to that used earlier (see [7], Fig. 1). The plasma jet from the EPG, after bursting a separating diaphragm, enters a tube, evacuated to 0.1 N/m^2 , of diameter 1 cm and length 4 cm, and a cylindrical glass bottle of diameter 9 cm and length 15.6 cm, and is decelerated at its end. The flight and deceleration of the plasma jet are recorded behind a violet filter with an effective wavelength of 432 nm and a half-width of 20 nm, using a type SFR-2M recorder. The brightness temperatures were determined by photometric comparison of the brightness of the test object and a type EV-45 standard source [5]. The presence at the step was measured by three piezoelectric sensors [4], located at different distances from the center of the step. The radiative fluxes emerging from the deceleration region were measured by glass plates with sintered strips of aluminum of known thickness. We recorded the times of appearance of light at the place where the aluminum strips evaporated under the influence of the radiation, and used the experimental correlation of [4] for the aluminum mass removed from the surface as a function of the radiative incident energy. Plates 1 to 3 were located at distances of 13.5-5.0, and 1.5 cm from the step.

Numerical modeling of the process investigated, the operation of the generator, and the impact of the high-speed plasma jet on the step was conducted using the theoretical model of the EPG [8-11], including a description of the detonation, launching of the plate due to explosion products, and the two-dimensional gasdynamic flow of the plasma in the compression chamber, exit tube and bottle, accounting for transport of the self-radiation and evaporation of the walls confining the plasma. For the explosion products, the air plasma and the aluminum vapor, we used the equations of state that allowed for real properties [12-14]. The spectral nature of the radiation was taken into account in the three-spectral-group approximation, within which the absorption coefficient was assumed to be independent of frequency and equal to the mean Planck spectral absorption coefficient.

In the process of operation of the generator the detonation wave, after passing along the explosive charge, accelerates the plate up to 4 km/sec at a distance of about 2 mm in a time of 3 μsec . Later the plate velocity reaches 5.5 km/sec, and close to the exit tube it falls sharply due to the counterpressure of the air compressed in the working chamber. It is compressed in the cavity of the spherical segment by 2 or 3 shock waves [8, 9, 11], and here the gas pressure can reach $\sim 1000 \text{ GN/m}^2$, the density $\sim 10 \text{ g/cm}^3$, and the temperature 250-350 kK [10]. In some cases the plate may be prematurely stopped before it reaches the exit aperture (to the tube), and consequently the plate and the chamber wall can be deformed. In addition, this may also be the cause of plasma loss when the plate is directed backwards or collapses in "pockets" formed by the curved surfaces of the plate and the segment. As was shown in [10], the nature of deceleration of the projectile depends on a number of factors:

Moscow, Minsk. Translated from Zhurnal Prikladnoi Mekhaniki i Tekhnicheskoi Fiziki, No. 4, July-August, 1986. Original article submitted June 21, 1985.

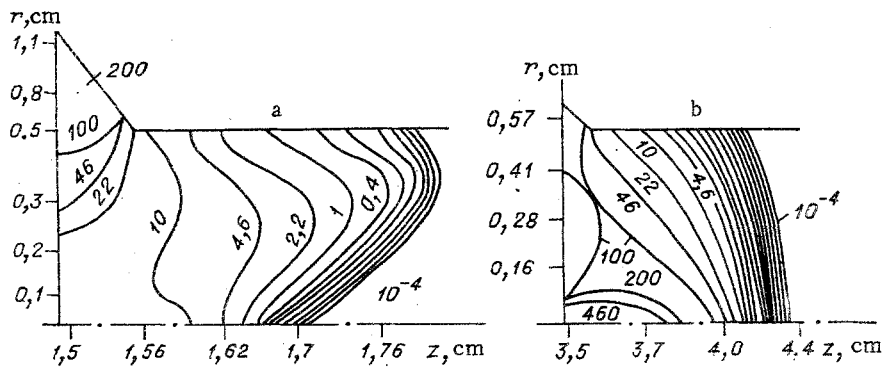


Fig. 1

the mass of gas and vapor reaching the wall, the radius of curvature of the segment, and so on.

Figure 1 shows the pressure distribution (the numbers on the isobars are given in GN/m^2) over the volume of the compression chambers of radius $R = 8$ and 5 cm (a and b), with identical sizes of the explosive and the plates initially (in the $R = 8$ cm case the initial mass of air in the chamber was 0.07 g). In Fig. 1a the plate was observed to come to rest at an earlier stage of compression, when the plasma had not fully emerged from the angle formed by the walls of the plate and the spherical segment. The total plasma energy, with the same jet velocity in the tube (64 and 65 km/sec) was 57 and 135 kJ in the experiment [7] and as calculated, respectively. This difference is probably due to the above-mentioned losses of the plasma. In case b the measured and calculated values of velocity at the step were 59 km/sec for total energy values of 110 and 116 kJ.

It can be seen in Fig. 1b that here the plate has almost fully reached the aperture of the exit tube (the scale along the z and r axes is irregular, and the true distance to the aperture is 0.2 mm). At that moment the largest values of pressure, density and temperature and the axial component of the mass velocity are reached on the symmetry axis, and at the maximum are $p \approx 700$ GN/m^2 , $\rho \approx 4$ g/cm^3 , $T \approx 174$ kK, $u \approx 20$ km/sec (on Fig. 2 p is 10^2 GN/m^2 T is $1/11.6$ kK [sic]).

As can be seen from Fig. 3 (lines 1-4 for $t = 13.5; 14.3; 14.9; 16$ μsec), in the flight of a compacted cluster (see Fig. 1b) into the evacuated tube and bottle for $R = 5$ cm the initial distribution of the specific kinetic energy $v^2/2$ over the jet mass m is quickly altered ($t \gtrsim 14$ μsec) in such a way that its forward part, having small mass, is accelerated continuously until it collides with the end of the bottle ($t < 16$ μsec). The massive part of the jet (more than $2/3$ of the total mass) decelerates mainly due to expansion of the cluster which initially had the maximum velocity. Where there is good agreement between the theoretical (solid lines) and experimental data (broken lines) over the high-speed part of the jet (Fig. 3) we note a considerable difference in theory and experiment in the value of the total mass of the jet (0.3 and 1.2 g), which indicates a need for supplementary investigation of a mechanism for increased ingress of wall material into the jet.

When the jet discharges into the bottle, theoretically and experimentally we observe a radial expansion of the jet with velocities of 25 and 20 km/sec. During deceleration of the flow on the side wall of the cylinder, a side reflected shock wave II is formed, moving at a certain angle to the symmetry axis. From Fig. 4, which shows the scheme for development of shock waves I-III for $t = 20, 22, 24, 26,$ and 28 μsec (lines 1-5) inside the bottle for the EPG jet variant with $R = 5$ cm, it can be seen that compression of the flow behind the side shock wave II leads to delay of jet reflection from the end of the bottle at $t > 20$ μsec . Because of the two-dimensional nature of reflection of the EPG jet in the bottle two fronts I and II are formed, moving along the z axis and along the bottle generator with different velocities and, along with the side wave II, forming a three-wave configuration (Fig. 4a-c). This structure decays at $t > 30$ μsec (Fig. 4c) into two waves perpendicular to the symmetry axis.

Comparison of the theoretical and experimental data (Fig. 5, solid and broken lines) shows satisfactory agreement between theory and experiment in regard to the pressure at the center of the step p and the velocity of the incident jet v , and the trajectory of the wave h

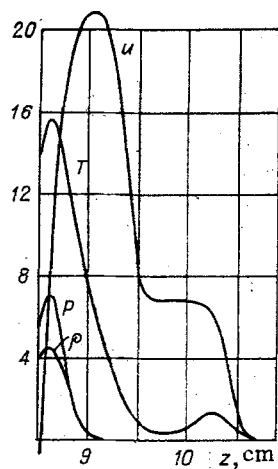


Fig. 2

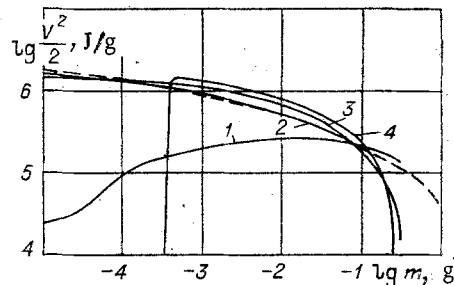


Fig. 3

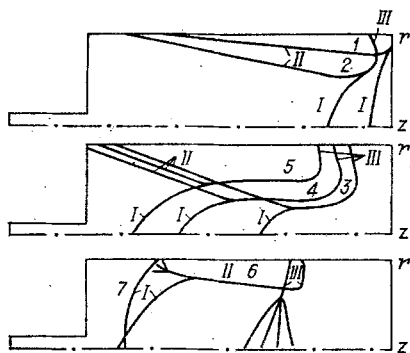


Fig. 4

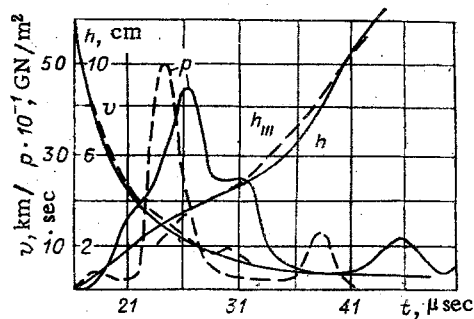


Fig. 5

observed in the experiment agrees well with the trajectory h_{III} , moving at the side wall. In this case the plasma in the bottle is optically dense, and therefore the position of the shock waves I and II were not recorded in the experiment.

The brightness temperatures at the step are 60 and 45 kK at the maximum, from the measured values directly and at 45° . The radiative energy fluxes emitted from the deceleration region reach 7.8, 50, and 150 MW/cm² in plates 1-3 at $t \approx 30 \mu\text{sec}$. The radiative output from the shock-compressed layer estimated from the results of measurement in this case did not exceed 3.5 kJ, which is 4% of the hydrodynamic energy of the jet. It was recorded that when the jet density was varied in the range $8 \cdot 10^{-6} - 4 \cdot 10^{-5} \text{ g/cm}^3$, due to further expansion of the jet, the maximum radiative fluxes were reduced to 30 MW/cm², but up to 60-77% of the hydrodynamic energy of the part of the jet having velocity above 10 km/sec is converted into radiative energy, which also agrees well with theory [9, 11].

The agreement of the experiment with the theory confirms the validity of the results of [3, 4, 7] and the correctness of the theoretical model of the EPG [8-11].

The authors thank V. I. Nemchinov for discussions and support in this work.

LITERATURE CITED

1. A. E. Voitenko, "The production of high-speed gas jets," Dokl. Akad. Nauk SSSR, No. 6 (1964).
2. A. E. Voitenko, E. P. Matochkin, and A. F. Fedulov, "An explosive tube," Prib. Tekhn. Eksp., No. 2 (1970).
3. Yu. N. Kiselev, and B. D. Khristoforov, "An explosive source of high-power continuum radiation," Fiz. Gor. Bzv., No. 1 (1974).
4. Yu. N. Kiselev, B. D. Khristoforov, and M. A. Tsikulin, "An experimental investigation of the action on a step of sources of high-power continuum radiation," in: The Low Temperature Plasma in Space and on Earth [in Russian], VAGO, Moscow (1977).
5. M. A. Tsikulin, and E. G. Popov, The Radiative Properties of Shock Waves in Gases [in Russian], Nauka, Moscow (1977).

6. V. I. Kirko, "The action of a high-enthalpy plasma, obtained with the aid of an explosive source, on the inside surface of a cavity and a channel," *Fiz. Gor. Vzv.*, No. 6 (1978).
7. Yu. N. Kiselev, K. L. Samonin, and B. D. Khristoforov, "Parameters of a jet for an explosive plasma compressor," *Zh. Prikl. Matem. Teor. Fiz.*, No. 3 (1981).
8. G. S. Romanov and V. V. Urban, "Numerical modeling of an explosive plasma generator in the gasdynamic approximation," *Inzh-Fiz. Zh.*, Vol. 37, No. 5 (1979).
9. G. S. Romanov and V. V. Urban, "Theoretical model of an explosive plasma generator," in: *Dynamics of Continuous Media. Unsteady Problems of Hydrodynamics* [in Russian], IG SO Akad. Nauk SSSR, No. 48 (1980).
10. G. S. Romanov, and V. V. Urban, "Numerical modeling of an explosive plasma generator, allowing for transfer of radiative energy and evaporation of the walls," *Inzh.-Fiz. Zh.*, Vol. 43, No. 6 (1982).
11. V. V. Urban, *A Theoretical Model of an Explosive Plasma Generator. Avtoref. Kand. Dis., NII PFP, Minsk* (1981).
12. V. F. Kuropatenko, "Equation of state of the products of detonation of condensed explosives," *ChMMSS*, Vol. 8, No. 6 (1977).
13. N.N. Kalitkin, and L. V. Kuz'mina, *Tables of Quantum Statistical Equations of State of Eleven Elements* [in Russian], Dep. VINITI, No. 2192-75, Moscow (1975).
14. N. M. Kuznetsov, *Thermodynamic Functions and Shock Adiabats for Air at High Temperature* [in Russian], *Mashinostroenie*, Moscow (1965).

MECHANISM OF SPACE CHARGE GENERATION IN SHOCK

COMPRESSION OF IONIC CRYSTALS

V. K. Sirotkin and V. V. Surkov

UDC 534.222.2

During shock loading of solids (dielectrics, semiconductors, metals) electromagnetic phenomena such as electromagnetic radiation and emission, development of a current between the plates of a shortcircuited capacitor upon their compression, etc. occur [1-3]. In a phenomenological description of such processes the shock front is considered as a discontinuity on which polarization, dielectric permittivity, and conductivity of the material are given, and the mechanism of charge liberation in the shock front is not concretized [1]. The present study will employ a different approach, based on study of the kinetics of point defects and dislocations in a shock front and will calculate the dependence of the change in potential (or polarization) over front width on the amplitude of shock compression, explaining a number of experimentally observed dependences. The materials which have been most studied at present are ionic crystals having an NaCl-type structure, in which the charge carriers are positive ion vacancies under normal circumstances. Electrification of crystals upon quasistatic loading (the Stepanov effect) is related to displacement of charged dislocations. In shock compression experiments the velocity and charge of the dislocations have different values, so that the role of dislocations in charge formation within the shock front is not known [1]. Attempts at explaining the effect in terms of diffusion of Na^+ vacancies through the shock front do not produce quantitative agreement with experiment [1]. The present study will examine both diffusion and over-barrier mechanisms of point defect and dislocation displacement with consideration of their multiplication in the shock front.

In the shock front multiplication of Frenkel defects occurs ($\sim 10^{17} \text{ cm}^{-3}$ per percent plastic deformation), so that interstitial ions also take on an important role. Lattice compression in the shock front leads to distortion of the equilibrium atomic configuration in the vicinity of a defect, as a result of which the latter may be displaced. Given a thermofluctuation mechanism, the probability that a defect of the k -th type will move from one equilibrium position to another is given by the expression